Quantitative Voltammetry in Weakly Supported Media. Chronoamperometric Studies on Diverse One Electron Redox Couples Containing Various Charged Species: Dissecting Diffusional and Migrational Contributions and Assessing the Breakdown of Electroneutrality

Juan G. Limon-Petersen, Jeongmin T. Han, Neil V. Rees, Edmund J. F. Dickinson, Ian Streeter, and Richard G. Compton*

Department of Chemistry, Physical and Theoretical Chemistry Laboratory, Oxford University, South Parks Road, Oxford, OX1 3QZ United Kingdom

Received: October 10, 2009; Revised Manuscript Received: December 4, 2009

Chronoamperometric transients are recorded in different quantities of supporting electrolyte, from full to self-support, for one electron transfer reactions of redox systems carrying diverse charges, and are studied to dissect migrational and diffusional contributions to mass transport under different conditions (applied overpotential, electrode radius, kinetics and charge of electroactive species). The one-electron redox systems studied are the reductions of Ru^{3+} (hexaammineruthenium(III)/(II)), Co^{3+} (cobaltocenium/cobaltocene), and Fe^{3+} (hexacyanoferrate(III)/(II)). The mass transport (diffusion and migration) is simulated using the Nernst−Planck−Poisson (NPP) model, with good agreement between experiment and theory. The effect of the charge of the electroactive species on its mass transport to the electrode is considered when only small amounts of supporting electrolyte are added to the solution. The mass transport to the electrode is increased by "attractive" migration when a positively charged electroactive species is reduced or a negatively charged species is oxidized. Conversely, when a positively charged electroactive species is oxidized or a negatively charged species is reduced, the migration is "repulsive" and the mass transport to the electrode is decreased.

1. Introduction

In an electrochemical reaction at the electrode−solution interface, charge is exchanged between the electrode and the electroactive species in solution; the resulting loss/gain of charge in solution is rapidly compensated by the movement of charged species within solution in a way that tends to dissipate the electric field.

A common practice is to add large quantities of charged species (supporting electrolyte) to the solvent to better disperse the charge created by the electrochemical reaction, and by doing so, avoid the creation of an electric field in solution that would cause voltammetric distortions. The appropriate amounts of supporting electrolyte required to avoid voltammetric distortions have been previously discussed.[1]

When an experiment lacks sufficient supporting electrolyte, the charged species present are not able to fully disperse the charge created by the electrochemical reaction. This causes a potential drop in the solution and transport by migration, resulting in distortions to the observed voltammetry and deviations from the behavior calculated for diffusion-only conditions. Quantitative voltammetry has been almost exclusively restricted to "supported" conditions although this creates an "artificial" medium in many cases. The interest for studying systems with low electrolytic support lies in the features and applications of electrochemistry under these conditions, for example to avoid complexation,[2] to study weak and strong acids,[3,4] disproportionation,[5,6] ion pairing,[7] biological systems, and for nonaqueous electrochemistry.[8] In addition, any study of electrochemical processes at the nanoscale requires a detailed understanding of coupled diffusion and migration.[9,10]

Previous studies have investigated some of the features of insufficient supporting electrolyte with the explicit assumption of electroneutrality, which is a reasonable approach under steady state conditions,[11−15] but lacks the necessary precision to study dynamic conditions such as apply in chronoamperometry or voltammetry. A recent study[16] has developed a computational strategy for the application of the full Nernst−Planck−Poisson system of equations for transient voltammetric conditions in which the constraint of electroneutrality has been removed. The model assumes that the structure of the double layer can be neglected (a discussion and validation of this assumption is presented elsewere[16]), and that the potential in solution varies from its value ϕ_{ref} in bulk solution to a value ϕ_{PET} at the site of electron transfer to or from the electrode (see Figure 1). The reaction of the electroactive species is assumed to occur at its closest approach to the electrode surface, which is referred to as the plane of electron transfer (PET) as shown in Figure 1. The potential drop in solution is defined $\Delta\phi_{PD} = \phi_{PET} - \phi_{ref}$, and the applied potential is defined $E = \phi_w - \phi_{ref}$, where ϕ_w is the potential of the working electrode.

Previous experimental and theoretical studies in our group have investigated weakly supported media using this model, for single and double electron transfer at amalgams[17,18] using hemispherical mercury drop electrodes, and with neutral electroactive species at a solid Au electrode.[19] Recently, experimental studies have achieved direct experimental evidence of migration.[20] In the present work we consider the impact of weak or zero support on a wide range of electrochemical systems, focusing exclusively on redox couples involving the gain of one electron, but examining a wide range of charges and

* Corresponding author. Fax: +44 (0) 1865 275410. Tel: +44 (0) 1865 275413. E-mail: richard.compton@chem.ox.ac.uk.

10.1021/jp9097149
Published on Web 01/14/2010

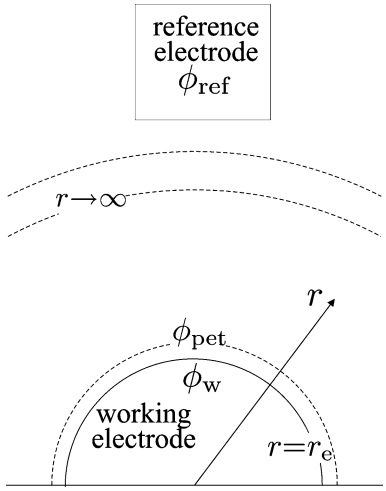

Figure 1. Diagram showing the boundary conditions used in the model.

comparing the experimental cases of cobaltocenium/cobaltocene in acetonitrile, hexaammineruthenium(III/II) in water, and hexacyanoferrate(III/II) in water, as shown below.

$$CoCp_2^+ + e^- \rightleftarrows CoCp_2 \quad (1)$$

$$[Ru(NH_3)_6]^{3+} + e^- \rightleftarrows [Ru(NH_3)_6]^{2+} \quad (2)$$

$$[Fe(CN)_6]^{3-} + e^- \rightleftarrows [Fe(CN)_6]^{4-} \quad (3)$$

We seek to provide a general understanding of the features induced by the absence of supporting electrolyte in solution by comparing and contrasting the differently charged electroactive species in order to derive new physical insights into the effects of coupled diffusion−migration as a function of species charge.

It is anticipated that the mass transport to the electrode is increased by "attractive" migration when a positively charged electroactive species is reduced. Conversely, when a negatively charged species is reduced, the migration is "repulsive" and the mass transport to the electrode is expected to decrease. Using the Poisson equation removes the constraint of electroneutrality, and so we are able to more accurately assess the manner in which the charge generated by the electrolysis is dispersed in solution. We find that contrary to the traditional point of view, deviations from electroneutrality are maintained at experimentally significant length and time scales.

2. Theoretical Model

In a recent study, Streeter et al.[16] applied the Nernst−Planck−Poisson system of equations to weakly supported voltammetry to simulate transient conditions and showed that there is no need to simulate the double layer to obtain reliable simulations under transient conditions for single potential step chronoamperometry, provided that the electrode is larger than nanoscale.[10] For the present study a similar model is used.

The following mechanism is modeled:

$$A^z + ne^- \rightleftarrows B^{z-n} \quad (4)$$

in which A and B are the electroactive species in solution, z is the charge of the initially present electroactive species and n is the number of electrons transferred. For this particular study, $n = +1$, and the reaction is supported by a concentration C_{sup} of a monovalent inert species M^+X^-. It should be noted that A and B are the same molecule, but are labeled differently for clarity of notation in the following sections.

The flux of the species in solution is modeled using the Nernst−Planck equation

$$\mathbf{J}_i = -D_i\left(\nabla C_i + \frac{z_i F}{RT} C_i \nabla\phi\right) \quad (5)$$

where for species i, $\mathbf{J}_i$ is the flux vector, D_i is the diffusion coefficient, C_i is concentration, z_i is the species charge, ϕ is potential, F is the Faraday constant, R is the gas constant, and T is the absolute temperature. The first term describes the contribution of diffusion to the flux and the second corresponds to the migration induced by electrostatic forces. The migration influences all of the charged species, so the simulation has to consider not just the electroactive species, but also the supporting electrolyte species. Convection effects are not considered and therefore our conclusions are only valid for short time scales following the beginning of the experiment (≤20 s).

To calculate the electric field in solution, the Poisson equation is solved simultaneously with the Nernst−Planck equation

$$\nabla^2\phi = -\frac{F}{\varepsilon_s\varepsilon_0}\sum_i z_i C_i \quad (6)$$

where ε_s is the dielectric constant of the solvent and ε_0 is the permittivity of free space.

The flux of a species as a function of time is then calculated by the continuity equation

$$\frac{\partial C_i}{\partial t} = -\nabla \cdot \mathbf{J}_i \quad (7)$$

These equations, the Nernst−Planck-Poisson equations, are solved in a 1D hemispherical space between an electrode with its plane of electron transfer (PET) at $r = r_e$. A Crank−Nicolson finite difference scheme is employed across irregular grids in space and time, and the iterative Newton−Raphson method is employed to solve the resulting set of nonlinear simultaneous equations. Full details, explanation of the numerical approach and references concerning numerical techniques have been reported in a previous study.[16]

The heterogeneous reaction rate at the electrode is controlled by the Butler−Volmer expression.

$$\left.\frac{\partial C_A}{\partial r}\right|_{r=r_e} = k^0\left(\exp\left(\frac{-\alpha F}{RT}(E - E_f^0 - \Delta\phi_{PD})\right)C_{A,0} - \exp\left(\frac{(1-\alpha)F}{RT}(E - E_f^0 - \Delta\phi_{PD})\right)C_{B,0}\right) \quad (8)$$

where $C_{i,0}$ is the concentration of the species i at the PET, E_f^0 is the formal potential of the couple, k^0 is the standard electrochemical rate constant, and α is the transfer coefficient. The other appropriate boundary conditions for the solution of these equations are as in Table 1.

TABLE 1: Boundary Conditions for the Simulation

Species/Potential	$r = r_e$	$r = r_e + 6(Dt)^{0.5}$
A	Butler−Volmer	$C_A = C_A^*$
B	$J_A = -J_B$	$C_B = 0$
M^+	$J_{M^+} = 0$	$C_{M^+} = C_{sup}(+ Z_A C_A^*$ if $Z_A < 0)$
X^-	$J_{X^-} = 0$	$C_{X^-} = C_{sup}(+ Z_A C_A^*$ if $Z_A > 0)$
ϕ	$(\partial\phi/\partial r) = 0$	$\phi + r(\partial\phi/\partial r) = 0$

3. Experimental Section

All aqueous solutions were made with ultra pure water with resistivity >18.2 MΩ cm at 298 K, and nonaqueous solutions were prepared with acetonitrile (MeCN, HPLC grade, Fisher Scientific).

Hexaammineruthenium(III) chloride (>98%, Aldrich), cobaltocenium hexafluorophosphate (>98%, Strem Chemicals), potassium hexacyanoferrate(III) (>98%, Aldrich), potassium nitrate (>99%, Aldrich), and tetra-butylammonium hexafluorophosphate (TBAP; >99%, Fluka) were used as purchased and without any further purification.

For this study, two different Pt planar working electrodes (WEs) of radii $r_e = 0.2$ cm and $r_e = 0.05$ cm were used (areas of 0.126 and 0.00785 cm^2, respectively). Two reference electrodes were used, depending on the solvent under study: a saturated calomel electrode for water and a Ag/Ag^+ electrode for MeCN (prepared in agreement with the procedure of Wain et al.[21]). A platinum wire of large surface area was used as a counter electrode. A μAutolab type III (EcoChemie, Utrecht, Netherlands) potentiostat was used throughout.

All solutions were thoroughly degassed with N_2 (BOC, High Purity Oxygen free) before starting each experiment and performed under thermostatic control at 298 ± 1 K using a water bath.

4. Results and Discussion

4.1. Theoretical Results. Single potential step chronoamperometry was simulated using the theoretical model described above: simulations were performed in which the working electrode is stepped from open circuit to a potential, E_1, at which electron transfer occurs rapidly, under two different concentrations of supporting electrolyte (Figure 2). The first system chosen for study was the single electron reduction of an electroactive neutral species with a formal potential set at $E_f^0 = 0$ V, and fast kinetics set as $k^0 = 1$ cm s^{-1}.

$$A + e^- \rightleftarrows B^- \tag{9}$$

This case was selected initially on the basis of it being the simplest to understand; more complicated cases will be examined in due course.

The additional parameters used for simulating the chronoamperometry are given in Table 2, together with a concentration of 600 mM supporting electrolyte, and an overpotential $E_1 - E_f^0$) of 250 mV. Figure 2 A shows the resulting current time response, which obeys the Cottrell equation[22] (which is an analytical solution for the purely diffusional flux to an electrode under fast kinetics), so proving the purely diffusional behavior of this simulation with respect to the electroactive species. The potential drop through the solution is very small compared to the applied overpotential, which is therefore approximately constant. There is negligible distortion to the concentration profiles of the supporting species compared to their bulk concentration. This is because high concentrations of supporting electrolyte confer the solution with high charge mobility compared to the charge exchanged at the interface. Therefore the exchanged charge is easily dispersed in the solution and the potential is almost constant throughout it.

Figure 2B shows another chronoamperogram, simulated as above, but with the supporting electrolyte concentration decreased to 0.3 mM. The solution does not possess such high levels of charged species, and when charge is exchanged between the electrode and the solution all the charged species are significantly attracted/repelled due to migration, modifying their concentrations and creating a potential drop through the solution. This potential drop is considerable and affects the rate of electron transfer. As time passes, the positively charged supporting species (i.e., that with opposite sign to the charge generated by the reaction) accumulates near to the electrode, reducing the local resistivity of the solution and increasing the potential difference experienced by the species at the PET. In turn this increases the observed rate of electron transfer, until mass transport (diffusion and migration) becomes rate limiting due to the depletion of electroactive species at the electrode surface. At this point the potential drop decreases considerably, due to the decrease of the flux of electroactive species to the electrode.

Figure 3 shows concentration profiles computed for the chronoamperogram in Figure 2 B. At a time of 10^{-3} s (t_a) the potential difference at the electrode interface ($\phi_{PET} - \phi_w$) is smaller than E_f^0 due to the potential drop in solution ($\Delta\phi_{PD}$). The electroactive species are in equilibrium at the interface, since kinetics are fast, but are equilibrated at a low interfacial potential difference compared to that applied (Figure 3, t_a), with a surface reactant concentration of 2.3 mM and product concentration of 0.5 mM. As the solution becomes negatively charged due to the reaction, the migrating positive ions concentrate near to the electrode, and the concentration of negative ions is reduced near to the electrode. As the reaction proceeds the local charge mobility in solution near the electrode increases because of the increased concentration of charged species (both electrolytically generated and supporting species). The potential difference at the interface increases due to reduced potential drop and the equilibrium between product/reactant then lies more to the product side, until the mass transport (diffusion and migration) due to the depletion layer becomes rate-limiting. At this point the potential drop through the solution lowers considerably. Then the negative ions disperse back to near to the electrode but the concentration of positive ions remains high (more than 8 times the bulk concentration) in order to disperse the charge exchanged at the interface.

Figure 3F shows the differences of the charge in solution with distance from the electrode, illustrating that the principle of electroneutrality is not followed. At short times following the potential step, the magnitude of the uncompensated charge in solution is about one tenth of the concentration of supporting electrolyte, and although previous studies[11−14] have used this electroneutrality approximation it is clear that it is not obeyed, and that even at relatively long times (t_e, 100 s) there is not exact electroneutrality within a distance of 10^{-3} cm from the electrode interface (Figure 3).

As previously explained, the potential drop through the solution decreases the actual potential difference at the interface, which also is a function on the overpotential applied to the system. The real applied potential ($\phi_w - \phi_{PET}$) reflects a balance between the current driven and the potential loss. The higher the potential applied between the electrode and the reference, the higher the potential applied at the interface, and therefore

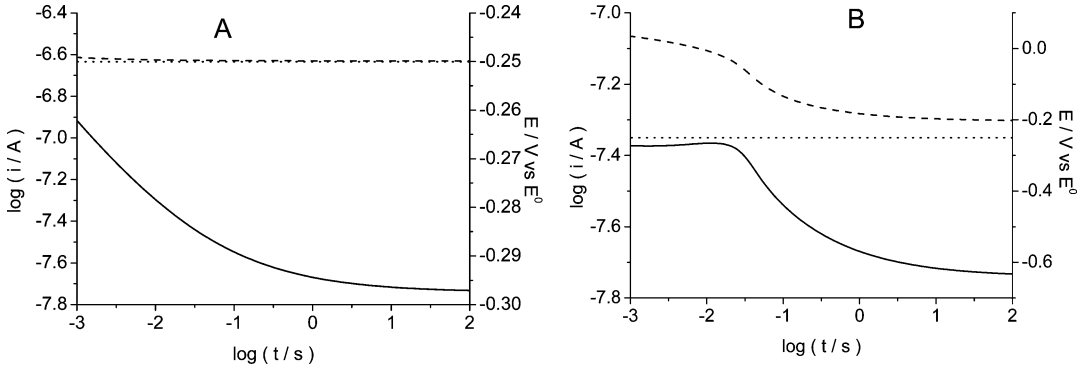

Figure 2. Simulated potential step chronoamperograms for a neutral electroactive species. In (A), there is a high support ratio $c_{sup} = 200$, and in (B) a low support ratio $c_{sup} = 0.1$. In both cases, $\Delta\phi_{PD}$, the potential difference arising between the reference and working electrodes (dashed line), and E, that applied, vs the reference electrode, at the working electrode (dotted line), are shown. The current−time response to the potential step is shown as a solid line.

TABLE 2: Values Used for the Numerical Simulation

parameter	value
C_A^*	3 mM
k^0	1 cm s^{-1}
D_A	1×10^{-5} cm^2 s^{-1}
D_B	1×10^{-5} cm^2 s^{-1}
D_{M^+}	1×10^{-5} cm^2 s^{-1}
D_{X^-}	1×10^{-5} cm^2 s^{-1}
r_e	1×10^{-3} cm

higher currents are expected causing greater potential drop through the solution (Figure 4).

It has been widely observed since the development of the microelectrode (see for example Montenegro[23] and references therein) that the potential drop is highly dependent on the electrode size.[24,25] Smaller electrodes are better able to disperse the charge in solution than large electrodes, and therefore their potential drop is smaller and the temporal region controlled by this potential drop is shorter. Figure 5B shows the variation of the potential drop with time, and it is clear that at small electrodes the potential drop decreases at a faster rate than for larger electrodes.

In Figure 5A, in the region ($t < 10^{-3.5}$ s) where the potential drop is the controlling factor ($E_f^0 > \phi_w - \phi_{PET}$), the current response is sensitive to the electrode kinetics. Where the kinetics are fast the potential drop has only to decrease a little to make a large change in charge transfer rate (and hence the observed current) whereas if the kinetics are slow a large change in potential drop gives only a very small difference in the rate of charge transfer. Consequently, one could observe kinetic effects, depending on the dispersion of the uncompensated charge (Figure 6). Using a small electrode the charge created by the reaction is dispersed faster and the effect on the chronoamper-

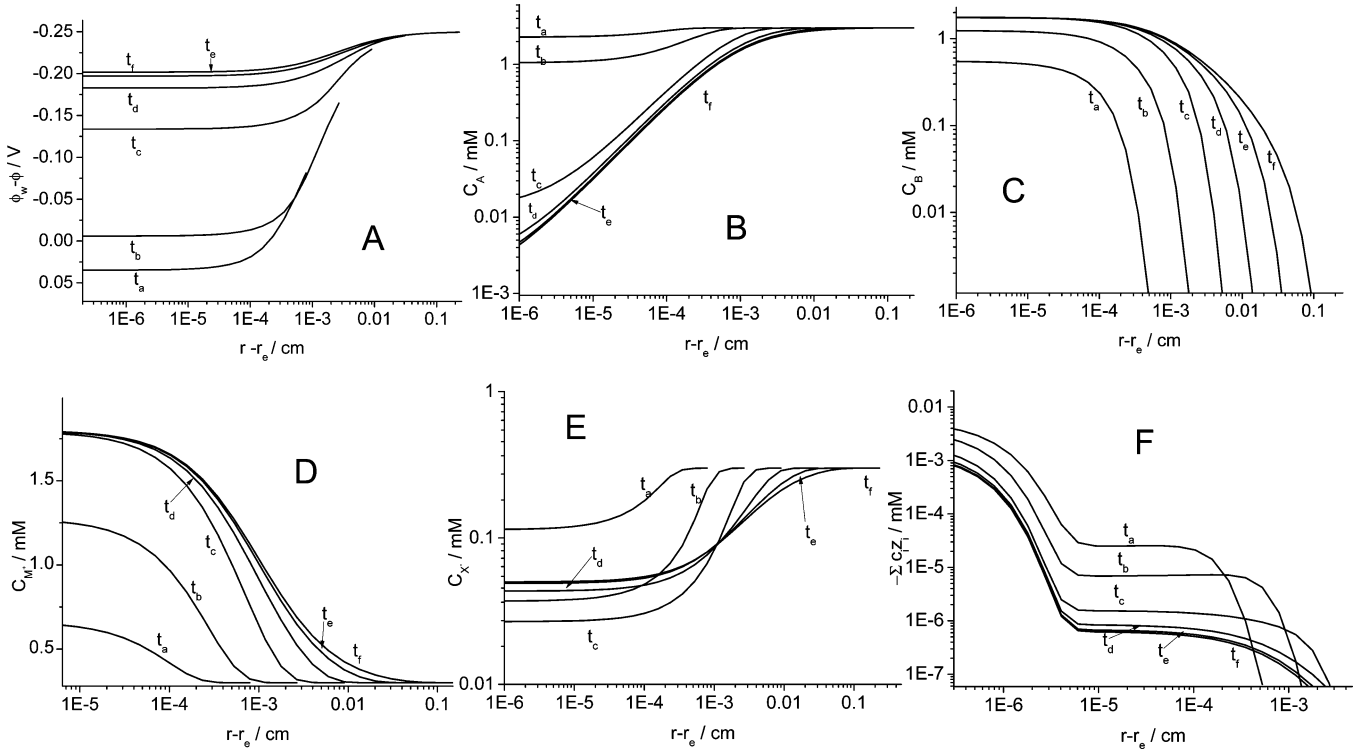

Figure 3. Simulated profiles for the chronoamperograms in Figure 2B at different times ($t_a = 10^{-3}$ s, $t_b = 10^{-2}$ s, $t_c = 10^{-1}$ s, $t_d = 1$ s, $t_e = 10$ s). (A) shows the variation of potential with distance from the electrode, and the other plots are concentration profiles of reactant (B), product (C), positive supporting species (D), negative supporting species (E), and uncompensated charge concentration (F).

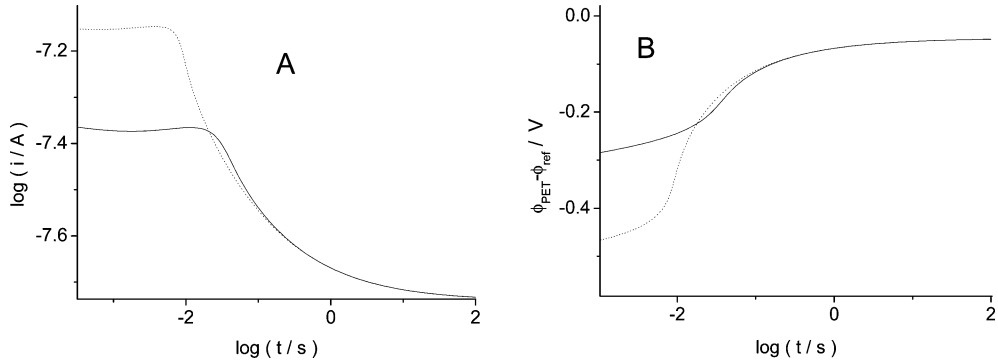

Figure 4. Simulated potential steps using the parameters in Table 2 with overpotentials of 200 mV (solid line) and 300 mV (dotted line). (A) shows the current transients and (B) the potential drop vs time.

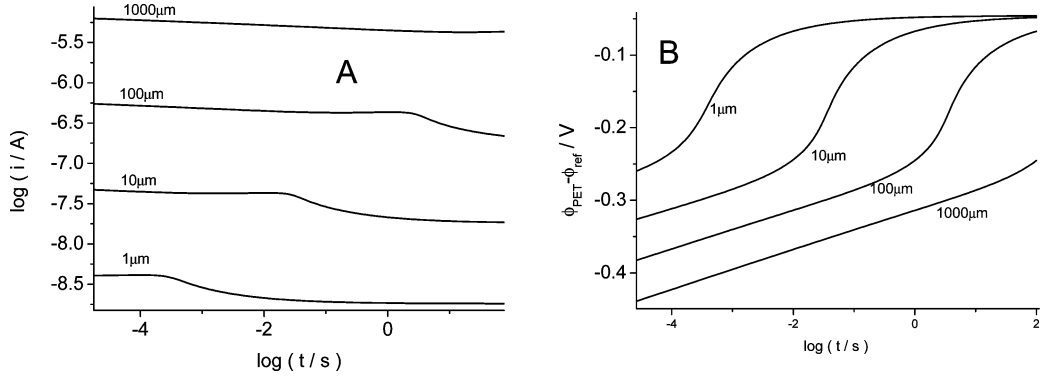

Figure 5. Simulated potential step responses with varying electrode size (radius stated on the figure). (A) Shows the current−time transient and (B) the potential drop vs time.

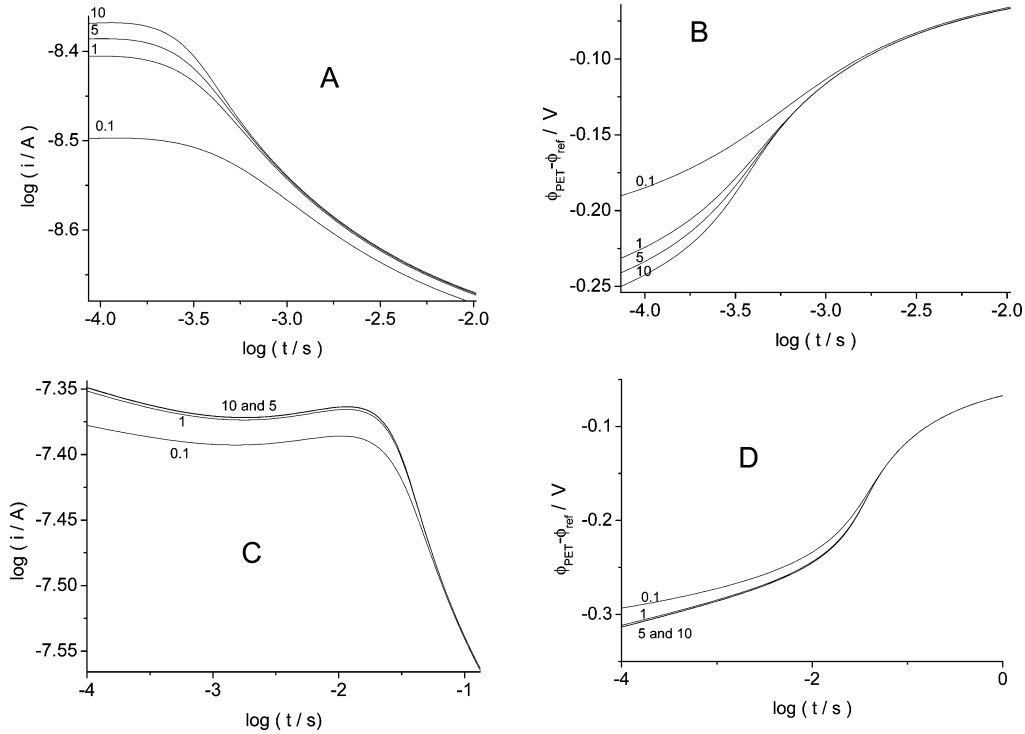

Figure 6. Influence of kinetics on weakly supported chronoamperometry for two different electrode radii 1 μm (A and B) and 10 μm (C and D), varying k^0 between 0.1, 1, 5, and 10 cm s^{-1} as stated in the image. (A) and (C) show current−time transients and (B) and (D) show potential drop vs time.

ometry due to kinetics is observable even at high values of k^0, whereas in larger electrodes these effects are negligible due to the slow rate of dissipation of charge.

Due to the charge transferred at the electrode surface, electrically charged species will migrate to distort the charge. The migration will be present in all systems, but if large amounts of supporting species are present compared to the quantity of electroactive species, the migration of the electroactive species can be small enough to consider that its transport approaches the purely diffusional limit. In a system with a low concentration

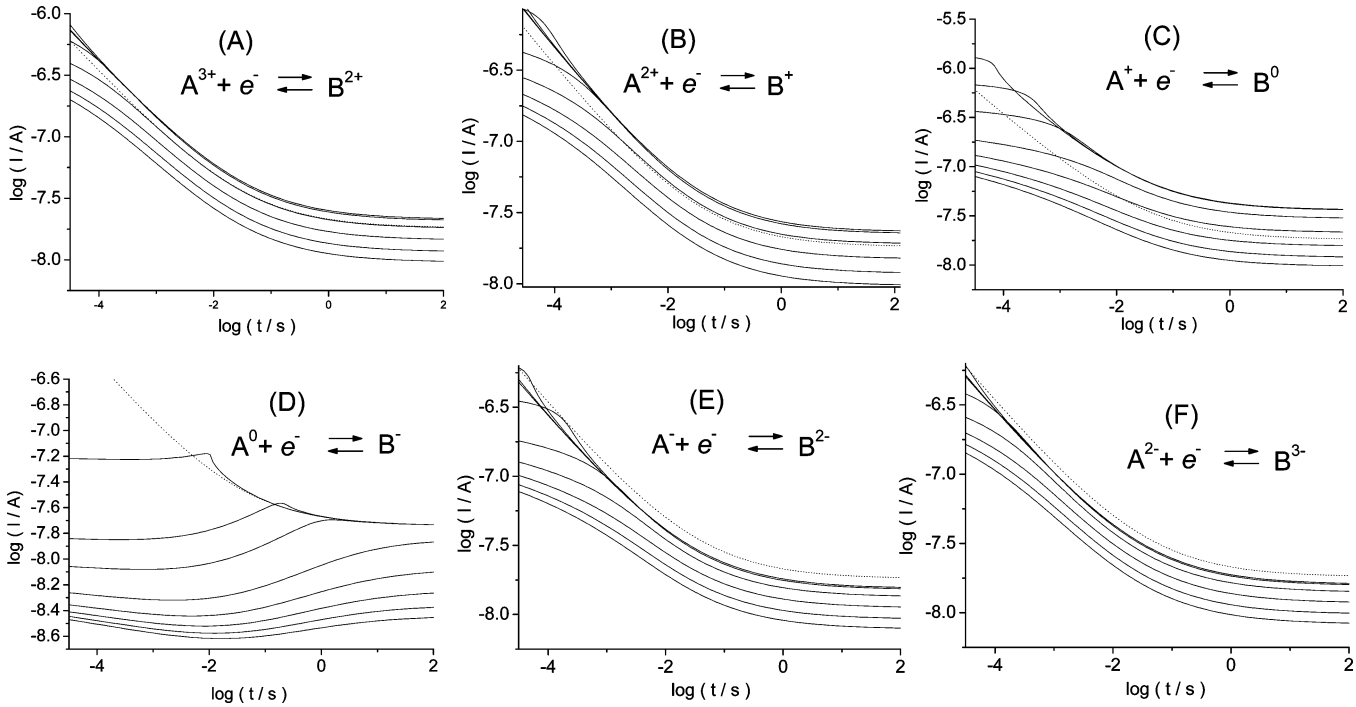

Figure 7. Potential steps for differently charged electroactive species over a range of applied overpotentials, E_1, of 0, 0.01, 0.025, 0.05, 0.1, 0.5, 1, and 2 V, compared with fully supported chronoamperometry (dotted line).

of supporting electrolyte, however, the added species are less able to distort the charge distribution and so the migration of the electroactive species will be comparable to its rate of diffusion. To explore this, the following part presents a study on differently charged electroactive species to obtain a general understanding of migration and potential drop under transient conditions. Chronoamperograms for different reductions are presented in Figure 7, each one with a differently charged electroactive species ($z = +3$, $+2$, $+1$, 0, -1, and -2, A−F respectively), simulated according to the parameters in Table 2, and with no extra supporting electrolyte except for Case D, where a supporting electrolyte concentration of 0.3 mM is input into the simulation, as the species is neutral.

While the following considers the case of electrochemical reduction, the results can be easily interpreted for oxidations because the key factor is the absolute charges on the reactant and product. For example, the reduction process that decreases the charge on the reactant from 2 to 1 gives numerically exactly the same current−time behavior, but with opposite sign, than the oxidation that increases the charge carried by another reactant from -2 to -1, and if the diffusion coefficients of all species are all equal, the electrostatic attraction and migration rates of all the species will be the same.

In the reduction of a positively charged electroactive species or the oxidation of a negatively charged electroactive species (Figure 7A−C), it is observed that the current is higher (solid lines) than for purely diffusional mass transport (dotted lines). Since the electroactive species has positive charge and the solution is accumulating negative charge (due to the reaction), the electroactive species is attracted by migration to the electrode, which increases its incident flux and hence the current.

In the case of a neutral electroactive species either being oxidized or reduced, its mass transport to the electrode remains purely diffusional as a neutral electroactive species cannot be attracted or repelled by migration (Figure 7D). This case exhibits a much more extensive potential drop effect, as it cannot be self-supported, and the concentration of added supporting ions in solution is much less than the concentration of counterions in the other cases. Certain unusual features of this extended potential drop regime for very weakly supported chronoamperometry, including minima in the observed Faradaic current, have been discussed previously.[19]

In the reduction of a negatively charged electroactive species or the oxidation of a positively charged electroactive species (Figure 7, panels E and F), the charge of the electroactive species has the same sign as the charge accumulated in solution. Therefore, repulsive migration will decrease the mass transport of the electroactive species to the electrode surface and the current is correspondingly decreased.

The steady state currents from the previous simulations are compared in Figure 8 with the values obtained by Oldham[14] with a good agreement between the NPP model and the electroneutral model at the limiting overpotential values.

Figure 8 shows that cases with less supporting electrolyte (less self-supporting electrolyte) have greater mass transport due to migration. For example, a electroactive species with charge of $+3$ under self-supported conditions (with 3 singly charged counterions), increases its mass transport to the electrode by 17%, but for the singly charged species with just a single counterion, the mass transport is increased by a factor of 200%.

4.2. Experimental Results and Discussion. In order to corroborate the theory, experiments were performed for different processes using standard electrochemical reagents known to display fast electron transfer, namely hexaammineruthenium(III) chloride, potassium hexacyanoferrate(III) and cobaltocenium hexafluorophosphate. Single potential step chronoamperometry was performed by stepping from open circuit to a potential, E_1, at which electron transfer occurs rapidly, and the current−time response was compared with simulated chronoamperograms produced according to the model previously described. Diffusion coefficients for the electroactive species were established by chronoamperometry, using the Cottrell equation, and by cyclic voltammetry at varying scan rate, using a Randles-Ševčík plot, both under fully supported conditions. In all of the simulations,

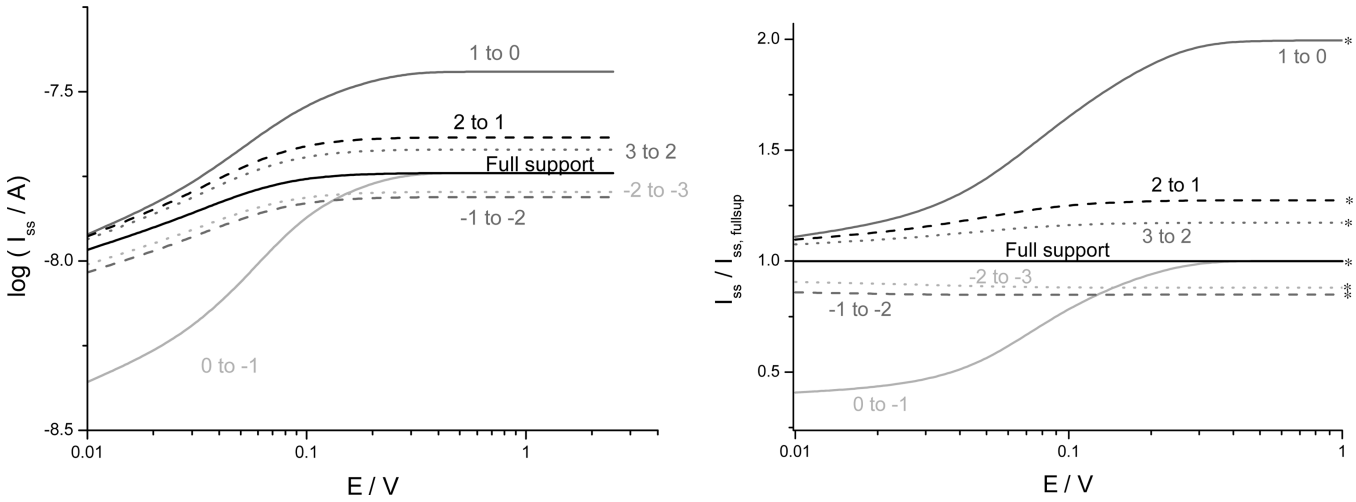

Figure 8. Steady state currents at different applied overpotentials for different electroactive species, and normalized (to full support currents) steady state currents. The limiting values are compared (*) with the previous study by Oldham[14] (see main text).

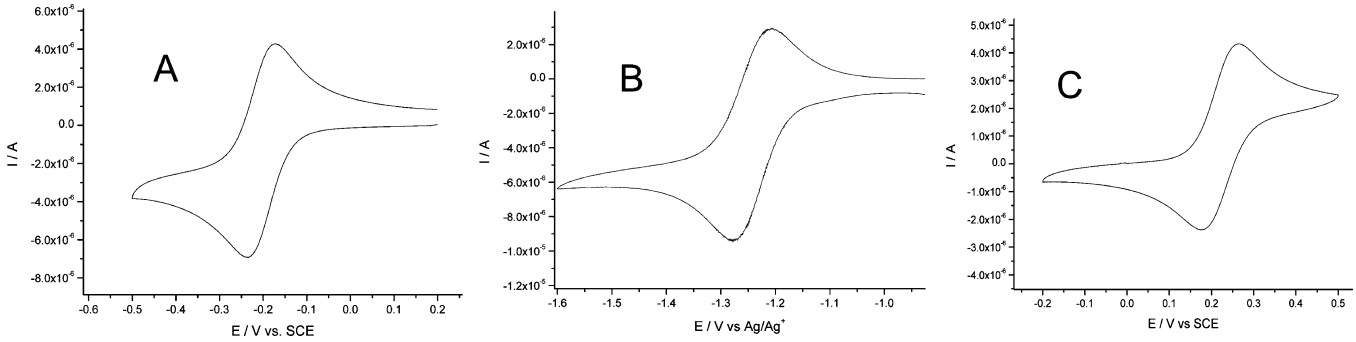

Figure 9. Cyclic voltammetry at a scan rate of 100 mVs^{-1} at a planar platinum electrode with $r_e = 0.5$ cm of (A) 3 mm hexaammineruthenium(III) chloride and 600 mM of potassium nitrate, (B) 3 mM cobaltocenium hexafluorophosphate and 600 mM of tetrabutylammonium hexafluorophosphate, and (C) 3 mM potassium hexacyanoferrate(III) and 600 mM of potassium nitrate.

it was approximated that the diffusion coefficients for the electroactive species at full support and those in the weakly supported solutions were equivalent; that is, that the effect of viscosity on the diffusion coefficients is negligible. Additionally, in all cases the planar Pt electrodes used experimentally were approximated as hemispheres of the same electroactive area, as justified in the procedure used previously by Dickinson et al.[1]

4.2.1. Hexaammineruthenium(III/II). First, cyclic voltammetry was performed using a platinum electrode in an aqueous solution containing 3 mM of hexaammineruthenium(III) chloride and 600 mM of potassium nitrate (i.e., fully supported conditions). A reversible cyclic voltammogram was obtained at a scan rate of 100 mV s^{-1} with a reversible peak-to-peak separation of ca. 60 mV (Figure 9), which enabled a formal potential, E_f^0, of −0.20 V (vs SCE) to be determined, which was found to be in agreement with literature values.[26,27] The diffusion coefficient was calculated by a Randles-Ševčík plot using cyclic voltammograms with scan rates of 100, 200, 500, and 1000 mV s^{-1}, and a value of 8.2×10^{-6} cm^2 s^{-1} obtained.

Next, chronoamperometry was performed in this solution using both sizes of platinum electrode, by stepping the potential from open circuit to −350 mV vs SCE (i.e., an overpotential of ca. 150 mV). The recorded chronoamperogram is shown in Figure 10 (in a logarithmic scale), and shows a typical diffusion-only response with a logarithmic gradient of −0.5 in accordance with the Cottrell equation. A value for the diffusion coefficient was determined from this plot to be 8.5×10^{-6} cm^2 s^{-1}, again in good agreement with literature values.[26,27]

Analogous chronoamperograms were recorded for solutions containing the same concentration of hexaammineruthenium(III) chloride but less supporting electrolyte (concentrations of 0 and 9 mM). Figure 10 also shows these data for both electrodes. Using the computational model described above, simulations were run using the experimental values for diffusion coefficient and formal potential, and other literature values listed in Table 3. These simulations were found to be in very good agreement with the experimental chronoamperograms, as indicated by the open circles in Figure 10. The transients recorded under highest support (600 mM) show purely diffusional behavior, whereas the weakly supported (30 mM) and self-supported transients exhibit at short time (10^{-2} s) a potential drop controlled region and at longer times ($t > 0.1$ s) a mass transport controlled region where current is enhanced by a factor of 1.12 by migration, as this is a reduction of a positively charged species(+3 to +2).

4.2.2. Cobaltocenium/Cobaltocene. Using the same methodology as described for the case of the reduction of hexaammineruthenium(III) chloride, cyclic voltammetry was performed in a solution containing 3 mM of cobaltocenium hexafluorophosphate and 600 mM of supporting electrolyte (TBAP) in acetonitrile. As before, a reversible cyclic voltammogram recorded at a scan rate of 100 mV s^{-1} is shown in Figure 9 with a peak-to-peak separation of 60 mV, which enabled a formal potential of −1.20 V (vs Ag/Ag^+) to be

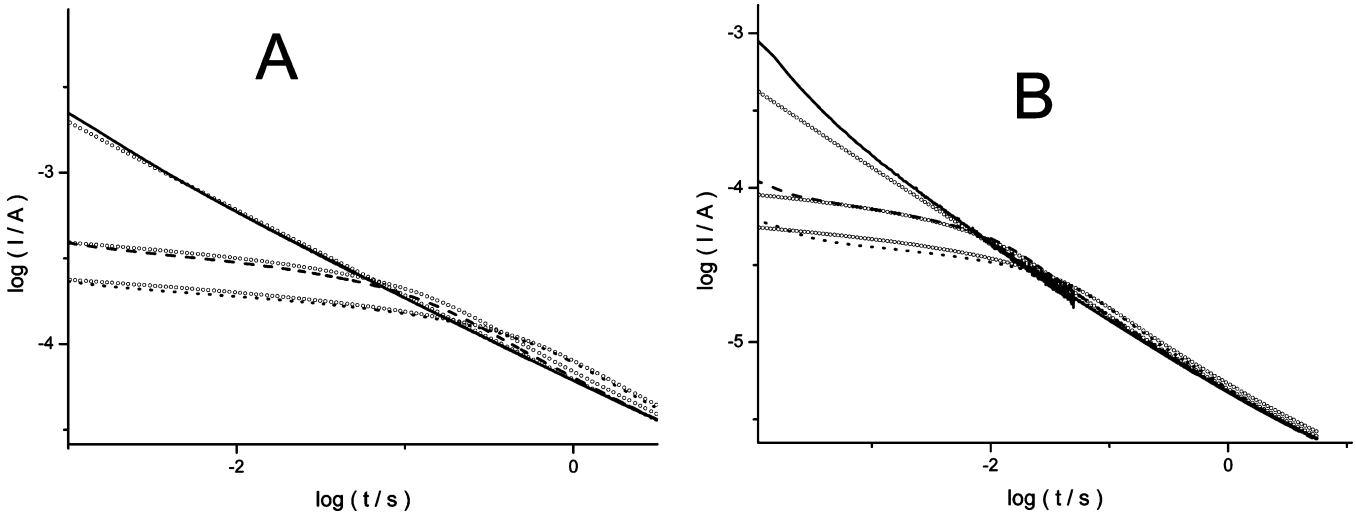

Figure 10. Comparison between experiment (lines) and simulation (circles) for the hexaammineruthenium(III/II) couple, with applied potentials of −0.350 V vs SCE and different concentrations of supporting electrolyte: 600 mM (line), 30 mM (dashed line), and self-supported (dotted). Comparison of different electrode radius: (A) 0.2 cm and (B) 0.05 cm.

TABLE 3: Values Used for the Comparison between Experiment and Theory

	hexaammineruthenium(III/II)	cobaltocenium/cobaltocene	hexacyanoferrate(III)/(II)
solvent	water	acetonitrile	water
E_f^0	−0.20 V vs SCE[26,27]	−1.2 V vs Ag/Ag$^+$ [29]	0.22 V vs SCE
k^0	0.7 cm s^{-1} [26,27]	1 cm s^{-1} [28]	0.6 cm s^{-1}
D_A	0.85×10^{-5} cm^2 s^{-1} [26,27]	2.3×10^{-5} cm^2 s^{-1} [29]	0.6×10^{-5} cm^2 s^{-1} [26,27]
D_B	0.85×10^{-5} cm^2 s^{-1} [26,27]	2.3×10^{-5} cm^2 s^{-1} [29]	0.6×10^{-5} cm^2 s^{-1} [26,27]
D_{M^+}	1.8×10^{-5} cm^2 s^{-1} [30]	3.0×10^{-5} cm^2 s^{-1} [a]	1.8×10^{-5} cm^2 s^{-1} [30]
D_{X^-}	1.8×10^{-5} cm^2 s^{-1} [30]	2.1×10^{-5} cm^2 s^{-1} [a]	1.8×10^{-5} cm^2 s^{-1} [30]

[a] Values estimated by the Wilke−Chang method.

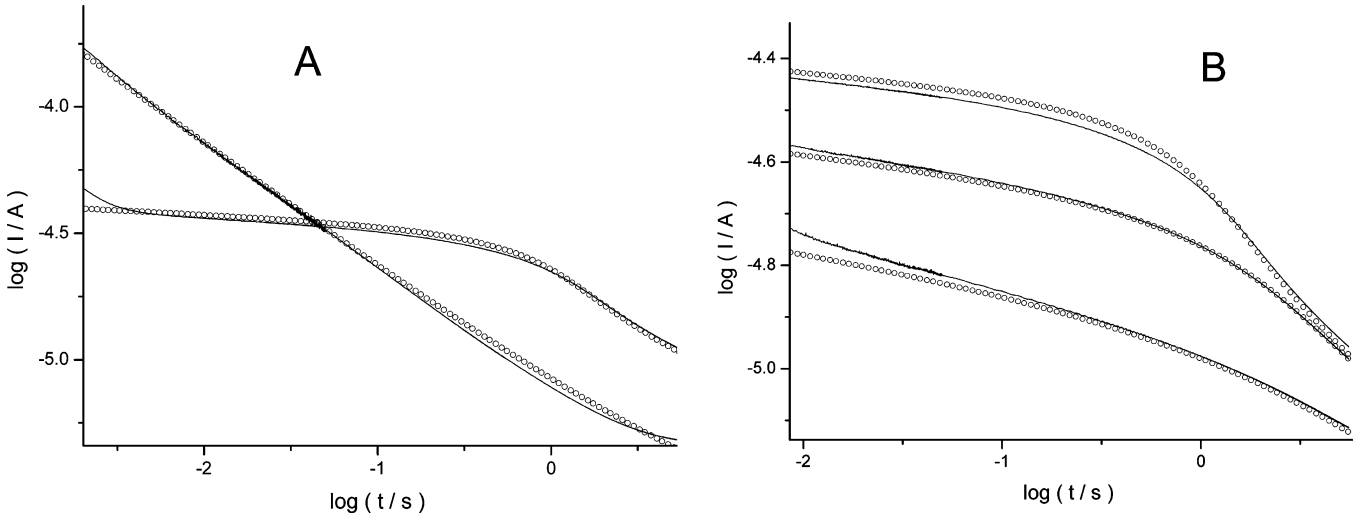

Figure 11. Comparison between experiment (line) and simulation (circles) for the cobaltocenium/cobaltocene couple. (A) Different concentrations of supporting electrolyte 600 mM and self-support and (B) different applied potentials (−1.30, −1.40, and −1.50 V vs Ag/Ag$^+$), without added supporting electrolyte.

determined. The diffusion coefficient calculated by a Randles−Ševčík plot for cyclic voltammograms with scan rates of 100, 200, 500, and 1000 mV s^{-1} was 2.0×10^{-5} cm^2 s^{-1}.

Then, single potential step chronoamperometry was carried out, stepping from open circuit to a potential of −1.50 V (vs Ag/Ag$^+$) (Figure 11 A). In the highest supported case (600 mM), a fully diffusional, Cottrellian-type response was obtained, which yielded a diffusion coefficient of 2.3×10^{-5} cm^2 s^{-1}. Both formal potential and diffusion coefficient were in good agreement with the literature.[28]

Similar chronoamperometric experiments were then carried out with zero added supporting electrolyte and also for potential steps to the potentials −1.30, −1.40, and −1.50 V (vs Ag/Ag$^+$) (Figure 11B). As before, the experimental results were compared with simulations undertaken using the parameter values listed in Table 3, assuming the diffusion coefficients to be independent

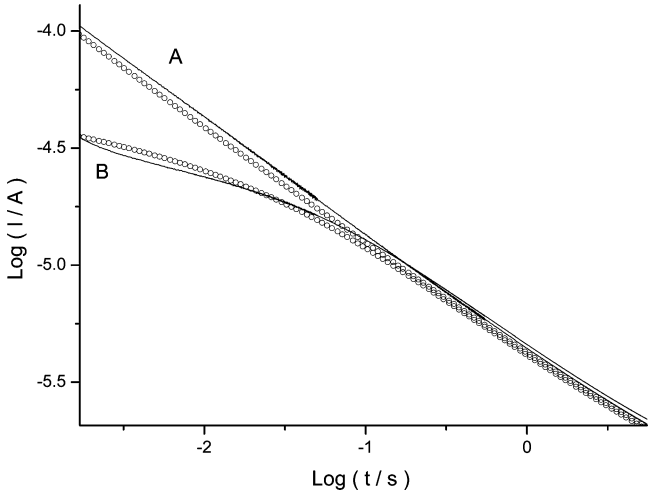

Figure 12. Comparison between experiment (line) and simulation (circles) for the hexacyanoferrate(III/II) couple, at an applied potential of +0.24 V vs SCE and different concentrations of supporting electrolyte: (A) 600 mM of supporting electrolyte and (B) self-supported.

of the supporting electrolyte concentration. Figure 11 shows the excellent agreement between experiment and simulation and the dependence of the current response in the potential drop region and applied overpotential.

In the self-supported chronoamperogram the mass transport is enhanced as cobaltocenium is positively charged and the reaction is a reduction. As cobaltocenium has just one counterion, higher migration rates than for hexaammineruthenium(III) are expected. It was found that under self-support conditions the steady-state current is enhanced by a factor of 2.80.

4.2.3. Hexacyanoferrate(III)/(II). Finally, the reduction of potassium hexacyanoferrate(III) was investigated. In fully supported solution containing 3 mM potassium hexacyanoferrate(III) and 600 mM of potassium nitrate, a reversible cyclic voltammogram was observed (Figure 9) which gave a formal potential of the redox couple to be +0.22 V (vs SCE). The diffusion coefficient was calculated by a Randles-Ševčík plot using cyclic voltammograms with scan rates of 100, 500, and 1000 mV s^{-1}, and a value of 6.4×10^{-6} cm^2 s^{-1} was obtained.

Chronoamperometry in this solution, stepping from open circuit to +0.52 V (vs SCE), gave a diffusional response for the high support case, enabling a value for the diffusion coefficient of 6.0×10^{-6} cm^2 s^{-1} to be determined. As before, formal potentials and diffusion coefficients agree well with literature.[26,27]

A chronoamperogram was recorded for the self-supported case (zero supporting electrolyte), and simulations conducted as described before. Figure 12 again shows that good agreement is observed between theory and experiment, and as this is the case of a reduction of a negatively charged electroactive species, the migration decreases the mass transport to the electrode (Figure 12).

4.2.4. Comparison. From the experimental observations described above, the strongest migrational influence is seen in the cobatocenium (+/0) system, in which the flux to the electrode is enhanced by migration by a factor of ca. 2.8 in self-supported long time transient conditions. For hexaammineruthenium (3+/2+), under self-support, an enhancement of long time transient flux of ca. 1.12 is presented compared to the purely diffusional case. The contrast between the two cases arises from the stoichiometry, since there is just one anion per ion of cobaltocenium, whereas for hexaammineruthenium(III) there are three. In the case of hexacyanoferrate(III) reduction, theory predicts a "repulsive" steady state migration effect of ca. 0.98, so that the experimental chronoamperograms for self- and full support essentially overlap. It should be noted that, although the overall effect of migration under transient conditions is common with that at steady state, a true steady state has not yet been attained and so the ratios presented differ from those calculated theoretically.[14] It is expected that at infinite time and in the absence of convective effects, the experimental transients would tend toward those limiting values.

The migration effects observed under self-supported conditions for a single electron transfer depend most strongly on the number of counterions associated with the electroactive species, since the extent of migration of the electroactive species reflects its proportion among all the charged species present in solution.

Conclusions

The NPP system of equations enables us to simulate with good agreement redox systems under different quantities of supporting electrolyte (support ratios of 0.1−200) for an electrode of size significantly greater than the nanoscale. The NPP model used here avoids the traditional approximation of electroneutrality.

The present study indicates that weakly supported chronoamperometry with microelectrodes could be used for electroanalytical research for obtaining kinetic parameters in self-supporting systems (Figure 6). This model has shown that the commonly used assumption of electroneutrality is weak since even at even at long time scales (up to 100 s) the solution is not electroneutral in a region up to 10^{-3} cm from the electrode (Figure 3).

We have demonstrated that the NPP equations combined with carefully selected boundary conditions are able to simulate different redox couples involving single step electron transfer, different species and concentrations of supporting electrolyte either in the steady state regime or under transient conditions. Mass transport (diffusion and migration) as predicted by the NPP model compared well with experiment. It is shown how the charge of the electroactive species affects its mass transport to the electrode when only small amounts of supporting electrolyte are added to the solution. The mass transport to the electrode is enhanced due to "attractive" migration, when low amounts of supporting electrolyte are used for a reduction of a positively charged species or an oxidation of a negatively charged electroactive species (Figure 7A−C). Conversely, when a positively charged electroactive species is oxidized or a negatively charged electroactive species is reduced, the mass transport to the electrode is reduced as the contribution of migration is "repulsive" (Figure 7, panels E and F). In the case of a neutral species under low supporting electrolyte conditions, its mass transport to the electrode will remain purely diffusional as neutral species do not migrate (Figure 7D).

Acknowledgment. J.G.L.P., N.V.R., and E.J.F.D. thank CONACYT, México, EPSRC, and St. John's College, Oxford, respectively, for funding.

References and Notes

(1) Dickinson, E. J. F.; Limon-Petersen, J. G.; Rees, N. V.; Compton, R. G. *J. Phys. Chem. C* **2008**, *113*, 11157–11171.

(2) Palys, M. J.; Rostek, E.; Stojek, Z. *Anal. Chim. Acta* **1998**, *377*, 29–37.

(3) Stojek, Z.; Ciszkowska, M.; Osteryoung, J. *Anal. Chem.* **1994**, *66*, 1507–1512.
(4) Aoki, K.; Baars, A.; Jaorski, A.; Osteryoung, J. *Anal. Chem.* **1994**, *66*, 1507–1512.
(5) Norton, J.; White, H. *J. Electroanal. Chem.* **1992**, *325*, 341–350.
(6) Norton, J. D.; Benson, W. W.; White, H. S.; Pendley, B. D.; Abruña, H. D. *Anal. Chem.* **1991**, *63*, 1909–1914.
(7) Watkins, J.; White, H. *Langmuir* **2004**, *20* (13), 5474–5483.
(8) Ciszkowska, M.; Stojek, Z. *J. Electroanal. Chem.* **1999**, *466*, 129–143.
(9) Conyers, J. L.; White, H. *Anal. Chem.* **2000**, *72* (18), 4441–4446.
(10) Dickinson, E. J. F.; Compton, R. G. *J Phys. Chem. C* **2009**, *113*, 17585–17589.
(11) Bento, M. F.; Thouin, L.; Amatore, C.; Montenegro, I. *J. Electroanal. Chem.* **1998**, *443*, 137–148.
(12) Hyk, W.; Stojek, Z. *Anal. Chem.* **2005**, *77*, 6481–6486.
(13) Bond, A. M.; Oldham, K. B.; Zoski, C. G. *Anal. Chim. Acta* **1989**, *216*, 177–230.
(14) Myland, J. C.; Oldham, K. B. *J. Electroanal. Chem.* **1993**, *347*, 49–91.
(15) Klymenko, O. V.; Amatore, C.; Svir, I. *Anal. Chem.* **2007**, *79*, 6341–6347.
(16) Streeter, I.; Compton, R. G. *J. Phys. Chem. C* **2008**, *112*, 13716–13728.
(17) Limon-Petersen, J. G.; Streeter, I.; Rees, N. V.; Compton, R. G. *J. Phys. Chem. C* **2008**, *112*, 17175–17182.
(18) Limon-Petersen, J. G.; Dickinson, E. J. F.; Rees, N. V.; Compton, R. G. *J. Phys. Chem. C* **2009**, *113*, 15320–15325.
(19) Limon-Petersen, J. G.; Streeter, I.; Rees, N. V.; Compton, R. G. *J. Phys. Chem. C* **2009**, *113*, 333–337.
(20) Amatore, C.; Knobloch, K.; Thouin, L. *Electrochem. Commun.* **2004**, *6*, 887–891.
(21) Wain, A. J.; Wildgoose, G. G.; Heald, C. G. R.; Jiang, L.; Jones, T. G. J.; Compton, R. G. *J. Phys. Chem. B* **2005**, *109*, 3971.
(22) Cottrell, F. G. *Z. Physik. Chem.* **1903**, *42*, 385–431.
(23) Montenegro, M. I. Applications of Microelectrodes in Kinetics. In *Research in Chemical Kinetics*; Compton, R. G., Hancock, G., Eds.; Elsevier: Amsterdam, 1994; Vol. 2.
(24) Beriet, C.; Pletcher, D. *J. Electroanal. Chem.* **1994**, *375*, 213.
(25) Jaworski, A.; Donten, M.; Stojek, Z. *Anal. Chim. Acta* **1995**, *305*, 106–113.
(26) Banks, C. E.; Compton, R. G.; Fisher, A. C.; Henley, I. E. *Phys. Chem. Chem. Phys.* **2004**, *6*, 3147–3152.
(27) Banks, C. E.; Rees, N. V.; Compton, R. G. *J. Electroanal. Chem.* **2002**, *535*, 41–47.
(28) Bowyer, W. J.; Engelman, E. E.; Evans, D. H. *J. Electroanal. Chem.* **1989**, *262*, 67–82.
(29) Tsierkezos, N. G. *J. Mol. Liq.* **2008**, *138*, 1–8.
(30) Harned, H. S.; Hudson, R. M. *J. Am. Chem. Soc.* **1951**, *73*, 652–654.

JP9097149